Nature and Strength of Metal−Chalcogen Multiple Bonds in High Oxidation State Complexes

Òscar González-Blanco,[†,‡] Vicenç Branchadell,[†] Kereen Monteyne,[‡] and Tom Ziegler*[,‡]

Departament de Química, Universitat Autònoma de Barcelona, Edifici Cn, 08193 Bellaterra, Spain, and Department of Chemistry, University of Calgary, Calgary, Alberta, T2N 1N4 Canada

Received May 22, 1997

Density functional theory calculations have been carried out on the trigonal complexes OsO_3E and MCl_3E (M = V, Ta) and the square pyramidal systems MCl_4E (M = Cr, Mo, W, Re) for E = O, S, Se, and Te as well as $(C_5H_5)ReO_3$. All complexes were fully optimized, and the calculated geometrical parameters are in reasonable agreement with gas-phase electron diffraction data where available. The calculated M−E bond energies decrease from oxygen to tellurium, from bottom to top in a metal triad, and from left to right in a transition series. The trend setting factor is the donation from the d_σ metal orbital to the p_σ acceptor orbital on the chalcogen atom. The contribution from the chalcogen to metal π back-donation has a maximum for sulfur and selenium. However in relative terms, the contribution from the π back-donation to the total M−E bond energy increases from oxygen to tellurium. Comparisons are made to previous calculations and experimental data on M−E bond strengths.

Introduction

Complexes with a multiple bond between a transition metal and a main group element have been studied extensively in recent years.[1,2] Efforts in synthesis and characterization have revealed a wide range of such compounds. Chief among them are those in which the main group element is a chalcogen. Complexes containing metal−oxygen multiple bonds have been the subject of a large number of investigations, and to some extent, metal−sulfur multiply-bonded complexes have also received attention.[3−5] On the other hand, interest in the homologous complexes of the heavier chalcogens, i.e. Se and Te, is just emerging[6−8] because of their potential use as precursors in the formation of thin-film semiconductors[9] and other solid-state materials.[8,10]

The body of experimental data available for metal−chalcogen complexes includes primarily spectroscopic properties as well as geometrical parameters obtained from solid-state[11] and gas-phase[12] studies. Experimental estimates of bond energies[13] are on the other hand rare. Theoretical studies[14] of metal−chalcogen complexes are also available, but again, they provide mainly structural and spectroscopic data. The structural and spectroscopic data generated so far have been used to provide tentative information about the order of the multiple metal−chalcogen bonds and the relative importance of the σ- and π-components.[15]

We present here a systematic study on the nature and strength of the bond between high-valent metal centers and the chalcogens E = O, S, Se, and Te. The metal centers are varied from the vanadium (VCl_3E and $TaCl_3E$) and chromium triads ($CrCl_4E$, $MoCl_4E$, WCl_4E) among early transition metals to $ReCl_4E$ and OsO_3E representing the middle to late transition metals. The relative contributions to the M−E bond from the σ- and π-components are analyzed by the extended transition state method.[16,17] Also included is $(C_5H_5)ReO_3$ since the first Re−O

[†] Universitat Autònoma de Barcelona.
[‡] University of Calgary.

(1) Nugent, W. A.; Mayer, J. M. *Metal-Ligand Multiple Bond;* Wiley: New York, 1988.
(2) Holm, R. H. *Chem. Rev.* **1987**, *87*, 1401.
(3) Griffith, W. P. *Coord. Chem. Rev.* **1970**, *5*, 459.
(4) Diemann, E.; Müller, A. *Coord. Chem. Rev.* **1973**, *10*, 79.
(5) Müller, A.; Diemann, E. *Comprehensive Coordination Chemistry;* Wilkinson, G., Gillard, R. D., McCleverty, J. A., Eds.; Pergamon: New York, 1987; Vol. 2.
(6) Roof, L. C.; Kolis, J. W. *Chem. Rev.* **1993**, *93*, 1037.
(7) Rabinovich, D.; Parkin, G. *J. Am. Chem. Soc.* **1991**, *113*, 9421.
(8) Christou, V.; Arnold, J. *J. Am. Chem. Soc.* **1992**, *114*, 6240.
(9) O'Brien, P. *Chemtronics* **1991**, *5*, 61.
(10) Cary, D. A; Arnold, J. *J. Am. Chem. Soc.* **1993**, *115*, 2520.
(11) See for example: (a) Ueki, T.; Zalkin, A.; Templeton, D. H. *Acta Crystallogr.* **1965**, *19*, 157. (b) Hess, H.; Hartung, H. *Z. Anorg. Allg. Chem.* **1966**, *344*, 157. (c) Drew, M. G. B.; Mandyczewsky, R. *J. Chem. Soc.* A **1970**, 2815. (d) Edwards, A. J. *J. Chem. Soc., Dalton Trans.* **1972**, 582.
(12) See, for example: (a) Palmer, K. J. *J. Am. Chem. Soc.* **1938**, *60*, 2360. (b) Seip, H. M.; Stølevik, R. *Acta Chem. Scand.* **1966**, *20*, 385. (c) Iijima, K.; Shibata, S. *Bull. Chem. Soc. Jpn.* **1974**, *47*, 1393. (d) Iijima, K.; Shibata, S. *Bull. Chem. Soc. Jpn.* **1975**, *48*, 666. (e) Page, E. M.; Rice, D. A.; Hagen, K.; Hedberg, L.; Hedberg, K. *Inorg Chem.* **1982**, *21*, 3280. (f) Hagen, K.; Hobson, R. J.; Rice, D. A.; Turp, N. *J. Mol. Struct.* **1985**, *128*, 33. (g) Page, E. M.; Rice, D. A.; Hagen, K.; Hedberg, L.; Hedberg, K. *Inorg. Chem.* **1991**, *30*, 4758. (h) Herrmann. *Inorg. Chem.* **1988**, *27*, 1254.
(13) (a) Glidewell, C. *Inorg. Chim. Acta* **1977**, *24*, 149. (b) Sanderson, R. T. *Inorg. Chem.* **1986**, *25*, 3518. (c) Bryan, J. C.; Mayer, J. M. *J. Am. Chem. Soc.* **1990**, *112*, 2298. (d) Conry, R. R.; Mayer, J. M. *Inorg. Chem.* **1990**, *29*, 4862. (e) Watson, L. R.; Thiem, T.; Dressler, R. A.; Salter, R. H.; Murad, E. *J. Phys. Chem.* **1991**, *95*, 8944. (f) Hildenbrand, D. L.; Lau, K. H. *J. Phys. Chem.* **1992**, *96*, 2325. (g) Holm, R. H.; Donahue, J. P. *Polyhedron* **1993**, *12*, 571. (h) Gable, K. P.; Juliette, J. J. J.; Gartman, M. A. *Organometallics* **1995**, *14*, 3138. (i) Gable, K. P.; Juliette, J. J. J. *Organometallics* **1996**, *15*, 5250.
(14) (a) Rappé, A. K.; Goddard, W. A., III. *J Am. Chem. Soc.* **1982**, *104*, 448. (b) Pershina, V.; Sepp, W.-D.; Bastug, T.; Fricke, B.; Ionova, G. V. *J. Chem. Phys.* **1992**, *97*, 1123. (c) Neuhaus, A.; Veldkamp, A.; Frenking, G. *Inorg. Chem.* **1994**, *33*, 5278. (d) Benson, M. T.; Cundari, T. R.; Lim, S. J.; Nguyen, H. D.; Pierce-Beaver, K. *J. Am. Chem. Soc.* **1994**, *116*, 3955. (e) Kaltsoyannis, N. *J. Chem. Soc., Dalton Trans.* **1994**, 1391. Pershina, V.; Fricke, B. *J. Phys. Chem.* **1995**, *99*, 144. (f) Cotton, F. A.; Feng, X. *Inor.g Chem.* **1996**, *35*, 4921.
(15) Pauling, L. *The Nature of Chemical Bond*, 3rd ed.; Cornell University Press: Ithaca, NY, 1960; pp 224 ff.
(16) Ziegler, T.; Rauk, A. *Theor. Chim. Acta* **1977**, *46*, 1.
(17) Ziegler, T.; Rauk, A. *Inorg. Chem.* **1979**, *18*, 1558.

S0020-1669(97)00613-7 CCC: $15.00
Published on Web 03/31/1998

Chart 1

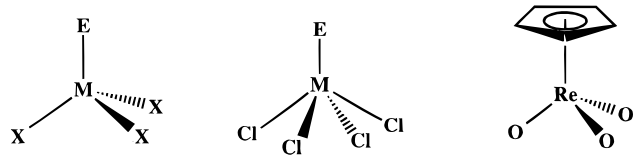

1 **2** **3**

dissociation energy is known experimentally with high accuracy for the related $(C_5Me_5)ReO_3$ system.

Computational Details

All the calculations are based on density functional theory[18−20] (DFT) and have been carried out using the Amsterdam density functional program[21] (ADF). The numerical integration procedure applied is due to te Velde and Baerends.[22] The molecular geometries have been optimized using the method developed by Versluis and Ziegler.[23] Gradient corrections (BP86) to the exchange[24] and correlation[25] were included self-consistently. An uncontracted triple-ζ basis of Slater type orbitals (STO's) was employed for the *n*s, *n*p, *n*d, $(n + 1)$s, and $(n + 1)$p valence shells of the transition metal elements and the *n*s,*n*p shells of the main group elements augmented with a set of polarization functions[26] for the non-metallic atoms. Inner shells have been treated by the frozen core approximation.[21b] Relativistic effects have been considered in all the atoms, in the so called *quasi-relativistic*[27,28] treatment, which means that the first-order scalar relativistic Pauli Hamiltonian is diagonalized in the space of the nonrelativistic solutions. An auxiliary[29] set of s, p, d, f, and g Slater-type functions centered on the nuclei has been used to fit the molecular density and to represent the Coulomb and exchange-correlation potentials accurately in each SCF cycle.

Results and Discussion

Optimized Geometries. The OsO_3E and MCl_3E (M = Ta, V) species were optimized under C_{3v} constraints, **1** (Chart 1), while the complexes MCl_4E (M = Re, W, Mo, Cr) were assumed to possess a square pyramidal C_{4v} conformation, **2**. For $CpReO_3$ no symmetry was assumed, **3**. Geometrical parameters for the optimized structures are displayed in Table 1.

The optimized M−E and M−Cl bond distances are generally longer than the available experimental estimates based on gas-phase electron diffraction studies.[12] The standard deviation for the M−Cl bonds is 0.05 Å compared to 0.06 Å for the M−E linkage. Bond angles are reproduced to within 2°. Our BP86 structures for the MCl_4E systems are in good agreement with the MP2 geometries obtained by Frenking[14c] et al. Cundari[14d] et al. have conducted the most comprehensive theoretical study on M−E bond lengths to date. They found that the M−E distances increase with nearly the same increments between two chalcogens independent of the metal center. This is also born out by the present investigation.

Table 1. Optimized Geometry Parameters[a,b] for the Complexes OsO_3E, MCl_3E (M = V, Ta), MCl_4E (M = Cr, Mo, W, Re), and $CpReO_3$

	O	S	Se	Te
Os−E	1.762 (1.711[c])	2.160	2.282	2.504
Os−O	1.762 (1.711[c])	1.768	1.769	1.771
E−Os−O	109.5 (109.4[c])	108.9	108.3	107.9
V−E	1.582 (1.56[d])	2.026	2.148	2.389
V−Cl	2.151 (2.12[d])	2.148	2.147	2.145
E−V−Cl	108.4 (108[d])	108.6	108.3	108.1
Ta−E	1.765	2.185	2.306	2.543
Ta−Cl	2.340	2.333	2.332	2.330
E−Ta−Cl	106.7	106.6	106.4	107.1
Cr−E	1.557	1.987	2.112	2.349
Cr−Cl	2.212	2.215	2.214	2.214
E−Cr−Cl	104.1	104.3	104.1	103.7
Mo−E	1.697 (1.658[e])	2.113	2.222	2.432
Mo−Cl	2.307 (2.279[e])	2.307	2.308	2.309
E−Mo−Cl	104.2 (102.8[e])	104.4	104.1	104.0
W−E	1.731 (1.685[f])	2.142 (2.086[g])	2.260 (2.203[g])	2.490
W−Cl	2.361 (2.280[f])	2.364 (2.277[g])	2.363 (2.284[g])	2.363
E−W−Cl	103.9 (102.4[f])	104.1 (104.2[g])	103.6 (104.4[g])	103.7
Re−E	1.716 (1.663[h])	2.117	2.235	2.458
Re−Cl	2.345 (2.270[h])	2.350	2.350	2.351
E−Re−Cl	106.0 (105.5[h])	105.9	105.2	105.1
Re−C(av)	2.50 (2.40[i])			
Re−O(av)	1.74 (1.70[i])			

[a] Distances in Å and angles in deg. [b] Available geometrical parameters from gas-phase electron diffraction studies are given in parentheses. [c] Reference 12b. [d] Reference 12a. [e] Reference 12d. [f] Reference 12c. [g] Reference 12e. [h] Reference 12f [i] Reference 12h based on $(C_5Me_4Et)ReO_3$.

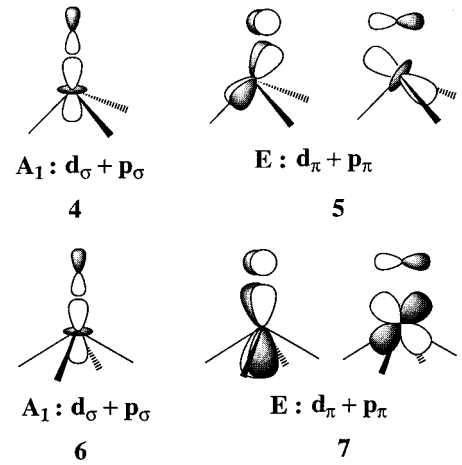

4 **5** **6** **7**

Figure 1. Orbital interactions in X_3ME, **4** and **5**, as well as Cl_4ME, **6** and **7**.

Metal−Ligand Interaction. The formation of the metal−ligand M−E bonds in **1** and **2** can be viewed as due to the interaction between a metallic fragment with 2 electrons in the d_{z^2} orbital of the metal and a chalcogen with its 4 valence electrons in the p_x and p_y orbitals, where the *z*-axis is directed along the M−E bond. These frontier fragment orbitals are represented in Figure 1, and their energies in the different compounds under consideration are shown in Figure 2. According to this model, the M−E bond is primarily due to a donation from the d_σ orbital of the metal to the p_σ orbital of the

(18) Parr, R. G.; Yang, W. *Density Functional Theory of Atoms and Molecules*; Oxford University Press: New York, 1989.
(19) Ziegler, T. *Chem. Rev.* **1991**, *91*, 651.
(20) Salahub, D. R.; Castro, M.; Proynov, E. Y. *Relativistic and Electron Correlation Effects in Molecules and Solids*; Malli, G. L., Ed.; Plenum Press: New York, 1994.
(21) (a) ADF, Department of Theoretical Chemistry, Vrije Universiteit, Amsterdam. (b) Baerends, E. J.; Ellis, D. E.; Ros, P. *Chem. Phys.* **1973**, 2, 41.
(22) te Velde, G.; Baerends, E. J. *J. Comput. Chem.* **1992**, *99*, 84.
(23) Versluis, L.; Ziegler, T. *J. Chem. Phys.* **1988**, *88*, 322.
(24) Becke, A. D. *Phys. Rev. A* **1988**, *38*, 3098.
(25) Perdew, J. P. *Phys. Rev. B* **1986**, *33*, 8822.
(26) Vernooijs, P.; Snijders, G. J.; Baerends, E. J. *Slater Type Basis Functions for the Whole Periodic System;* Internal Report; Freie Universiteit: Amsterdam, 1981.
(27) (a) Snijders, J. G.; Baerends, E. J. *Mol. Phys.* **1978**, *36*, 1789. (b) Snijders, J. G.; Baerends, E. J.; Ros, P. *Mol. Phys.* **1979**, *38*, 1909.
(28) Ziegler, T.; Tschinke, V.; Baerends, E. J.; Snijders, J. G.; Ravenek, W. *J. Phys. Chem.* **1989**, *93*, 3050.
(29) Krijn, K.; Baerends, E. J. *Fit Functions in the HFS Methods;* Internal Report; Freie Universiteit: Amsterdam, 1984.

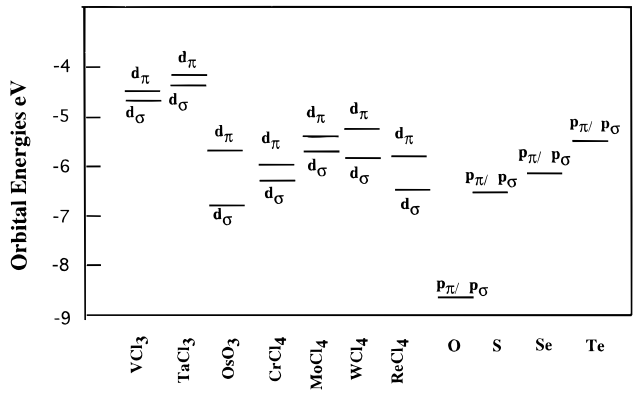

Figure 2. Orbital energy diagram for the d_σ and d_π levels of the metal fragments with the electron configuration $d_\sigma^2 d_\pi^0$ as well as the p_σ and p_π levels of the chalcogens with the electron configuration $p_\pi^4 p_\sigma^0$. The metal fragments MX_3 and MCl_4 have the same (deformed) structures as in X_3ME and Cl_4ME, respectively.

ligand, **4** and **6** of Figure 1, and a back-donation from the $p_{\pi(x)}$ and $p_{\pi(y)}$ orbitals of the ligand to the $d_{\pi(xz)}$ and $d_{\pi(yz)}$ orbitals of the metal, respectively, as shown in **5** and **7** of Figure 1. In general the σ-component of the M−E bond involves fragment orbitals of A_1 symmetry, including **4** and **6**, whereas the π-bond components are made up of E orbitals, including **5** and **7**.

The metal−chalcogen bonds in **1** and **2** can be analyzed in more quantitative terms by the extended transition state method[16,17] (ETS). The ETS scheme expresses the bonding energy between two fragments A and B as

$$BE = -(E_{\text{prep}} + E_{\text{st}} + E_{\text{orb}}) \qquad (1)$$

The first term, E_{prep}, is the energy needed to "prepare" the fragments for the M−E bond formation. In the case of the ligand, E_{prep} represents the energy needed to promote the chalcogen from its ^3P triplet ground state to the $(p_\sigma)^0(p_\pi)^4$ valence configuration. In the case of the metallic fragment, the same term includes a distortion from the geometry of the fragment in its ground state to its geometry in the combined compound as well as an electronic promotion to the $(d_\sigma)^2(d_\pi)^0$ valence state if this is not already the electronic ground state configuration of the metallic fragment.

The second term of eq 1 is referred to as the steric interaction energy between the two fragments A and B. It can in turn be expressed as

$$E_{\text{st}} = E_{\text{Pauli}} + E_{\text{elstat}} \qquad (2)$$

Here, E_{Pauli} represents the destabilizing 2-orbital−4-electron interactions between occupied orbitals of the two fragments in their prepared states. The contribution E_{elstat} of eq 2 represents on the other hand the total electrostatic interaction between the two prepared fragments at the positions they will take up in the combined complex.

The last contribution in (1) is the orbital term. It stems from the stabilizing 2-orbital−2-electron interactions between occupied and virtual orbitals of the two fragment in their prepared states. The orbital term can[16,17] further be split into contributions from the different symmetry representations as

$$E_{\text{orb}} = \sum_i E_{\Gamma_i} \qquad (3)$$

For the complexes **1** and **2**, E_{A_1} accounts for all the bonding σ-interactions, including **4** and **6** of Figure 1, whereas E_E represents the corresponding π-type interactions including **5** and **7** of Figure 1. Contributions from other symmetry representations are minute (<0.1 kJ/mol). Thus, eq 3 can be expressed as

$$E_{\text{orb}} = E_{A_1} + E_E = E_\sigma + E_\pi \qquad (4)$$

Table 2. Decomposition of the X_3M-E Bond Energy[a,b]

			O	S	Se	Te
OsO_3E	E_{prep}	E_{prep} E	66.4	40.8	37.0	31.8
		E_{prep} OsO_3	13.1	12.0	11.0	10.4
		total	79.5	52.8	48.0	42.2
	E_{st}	Pauli	329.1	219.3	198.2	159.9
		elstat	−125.8	−105.4	−103.6	−88.6
		total	203.3	113.9	94.6	71.3
	E_{orb}	E_σ	−341.9	−181.4	−148.0	−107.0
		E_π	−44.6	−60.1	−58.8	−57.2
		total	−386.5	−241.5	−206.8	−164.2
	BE		103.7 (104)[c]	74.8	64.2	50.7
VCl_3E	E_{prep}	E_{prep} VCl_3	27.2	27.5	27.1	26.9
		total	93.6	68.3	64.1	58.7
	E_{st}	Pauli	334.7	219.1	212.1	176.7
		elstat	−131.2	−111.4	−120.4	−109.8
		total	203.5	107.7	91.8	66.9
	E_{orb}	E_σ	−397.5	−216.9	−184.6	−140.4
		E_π	−50.9	−55.9	−55.1	−51.3
		total	−448.4	−272.8	−239.7	−191.7
	BE		151.3	96.8	83.8	66.1
$TaCl_3E$	E_{prep}	E_{prep} $TaCl_3$	11.9	11.5	11.3	12.1
		total	78.3	52.3	48.3	43.9
	E_{st}	Pauli	423.6	302.3	292.6	246.0
		elstat	−190.4	−184.1	−196.8	−180.8
		total	233.2	118.2	95.8	65.2
	E_{orb}	E_σ	−432.4	−236.8	−198.1	−148.8
		E_π	−56.1	−64.3	−63.1	−58.1
		total	−488.5	−301.1	−261.2	−206.9
	BE		177.0	130.6	117.1	97.8

[a] Values in kcal mol^{-1}. [b] The M−E bond energy BE is given as BE $= -(E_{\text{prep}} + E_{\text{st}} + E_{\text{orb}})$. [c] Experimental value from ref 13f.

Our decomposition analysis is not unique since it is based on a particular prepared state for the metal fragment and the ligand E. However, it is useful for a discussion of trends. Also, the final bonding energy, BE, does not depend on our choice of prepared valence state since corrections are added in the form of E_{prep}, eq 1.

MX_3E Complexes. The calculated M−E bond energies, BE, for the C_{3v} complexes OsO_3E and MCl_3E (M = V, Ta) with E = O, S, Se, and Te are presented in Table 2 along with the various terms from the ETS decomposition according to (1)−(4). It follows from Table 2 that the metal to ligand σ-donation contribution, $-E_\sigma$ of (4), in all cases is numerically more important for BE than the contribution $-E_\pi$ from the ligand to metal π back-donation.

The contribution, $-E_\sigma$, from the σ-donation as well as the total M−E bond energy is especially large for the most electronegative chalcogen, oxygen, as it has a p_σ orbital of much lower energy than the other group 16 elements, Figure 2. The sharp increase in the energy of p_σ between oxygen and sulfur, Figure 2, is reflected in a corresponding steep drop in both $-E_\sigma$ and BE, Table 2. By contrast, the p_σ acceptor orbital on sulfur is only slightly more stable than p_σ of selenium, resulting in a modest decrease for both $-E_\sigma$ and BE between these two elements. Tellurium is seen to form the weakest M−E bond, Table 2, as it has the p_σ acceptor orbital of highest energy. The larger decrease in BE between selenium and tellurium than between sulfur and selenium correlates well with the relative changes in the energy of p_σ between the same elements, Figure 2.

The contribution, $-E_\pi$, from the chalcogen to metal π back-donation increases from oxygen to sulfur and selenium as the p_π donor orbitals rise in energy and close the energy gap to the d_π metal acceptor orbitals, Figure 2. One might have expected $-E_\pi$ to reach a maximum for tellurium where the donor−acceptor energy gap is smallest. Instead $-E_\pi$ is seen to drop slightly compared to selenium as the diffuse $5p_\pi$ orbitals of tellurium form poorer overlaps with d_π than the more compact $4p_\pi$ orbitals of selenium. However, the contribution of the π-bonding components $-E_\pi$ to BE relative to that of $-E_\sigma$ is seen to increase from oxygen to tellurium. We note that the same trends in $-E_\pi$ and $-E_\sigma$ within the chalcogen family have been found previously in ETS studies of Cp_2ME (M = Ti, Zr)[30] and Me_3PE.[31]

The metal centers on the $TaCl_3$ and VCl_3 fragments belong to the top and bottom of the group 5 early transition metal triad. Early transition metals have a low electronegativity resulting in diffuse d-orbitals of high energy. The energy is further raised in metal complexes through antibonding interactions with the surrounding ligand orbitals augmented by the diffuse nature of the d-orbitals which results in large metal−ligand overlaps. This is particularly true for the 5d member tantalum which is seen to have the d_σ and d_π orbitals of highest energy, Figure 2. Osmium belongs to the bottom of the late group 8 transition metal triad. Late transition metals have a relatively high electronegativity resulting in compact d-orbitals of lower energy. Thus, OsO_3 has the d_σ and d_π orbitals of lowest energy, Figure 2. It is a general trend that metal−ligand overlaps for a given ligand decreases from bottom to top in a triad and from left to right in a transition series with a decreasing radial extent of the d-orbitals. On the other hand, for a given metal the metal−ligand overlap decreases within a family congeners such as the chalcogens with increasing *n*-quantum number as the p-ligand orbitals become more diffuse.

The trend in the d_σ energies provides $TaCl_3E$ with the largest $-E_\sigma$ contribution and the strongest M−E bond followed by VCl_3E and OsO_3E. The π-bonding component $-E_\pi$ does not vary much between the three metal fragments. Tantalum has the largest $-E_\pi$ contribution, although its d_π acceptor orbitals are of highest energy, because of the better $\langle d_\pi|p_\pi\rangle$ overlap arising from the diffuse nature of d_π for this element.

The chalcogen preparation energy from the ^3P to $(p_\pi)^4$ promotion decreases from oxygen to tellurium as the expansion of the *np* orbitals reduces the exchange stabilization between electrons of like spin, Tables 2 and 3. The geometrical preparation energies for the MX_3 fragments are relatively modest since the MX_3 ground-state conformation is close to that adopted by the same fragment in the MX_3E complex. The VCl_3 fragment needs in addition to be promoted from its triplet ground state ($d_\pi^1 d_\sigma^1$) to the d_σ^2 valence configuration whereas OsO_3E and $TaCl_3E$ both have a singlet (d_σ^2) ground state. The total destabilizing steric interaction energy, E_{st} of (2), decreases from oxygen to tellurium as the M−E bond becomes longer.

The three metal complexes examined here represent only a small cross section of the series of tetrahedral $MCl_{3-n}O_nE$ ($n = 0, 3$) complexes. However, on the basis of our analysis, we will predict that the M−E bond strength for a given chalcogen will decrease from bottom to top in a triad and from left to right within a transition series. The M−E bond energies within the chalcogen family should follow the same trend irrespective of the metal center. We note that FeO_4 with the predicted weakest M−O bond is, in fact, unknown. A Mulliken population analysis indicates further that the polarity of the M−E bond decreases with the M−E bond strength and is determined largely by the σ-donation.

Table 3. Decomposition of Me Cl_4M−E Bond Energy[a,f]

			O	S	Se	Te
$CrCl_4E$	E_{prep}	E_{prep} E	66.4	40.8	37.0	31.8
		E_{prep} $CrCl_4$	75.5	75.9	75.6	75.0
		total	141.9	116.7	112.6	106.8
	E_{st}	Pauli	287.4	184.3	170.9	138.6
		elstat	−86.0	−63.4	−65.8	−57.5
		total	201.4	120.9	105.1	81.1
	E_{orb}	E_σ	−341.6	−179.1	−150.1	−110.0
		E_π	−71.5	−82.4	−80.8	−77.0
		total	−413.1	−261.5	−230.9	−187.0
	BE		69.8	23.9	13.2	−0.9
$MoCl_4E$	E_{prep}	E_{prep} $MoCl_4$	45.0	45.2	44.9	44.7
		total	111.4	86.0	81.9	76.5
	E_{st}	Pauli	361.1	240.3	233.4	201.9
		elstat	−142.1	−116.9	−124.1	−114.7
		total	219.0	123.4	109.2	87.2
	E_{orb}	E_σ	−384.3	−203.0	−172.2	−130.1
		E_π	−72.1	−85.5	−85.5	−83.2
		total	−456.4	−288.5	−257.7	−213.3
	BE		126.1 (101)[b]	79.1	66.5	49.6
WCl_4E	E_{prep}	E_{prep} WCl_4	23.8	23.6	24.3	23.9
		total	90.2	64.4	61.3	55.7
	E_{st}	Pauli	396.5	270.3	255.4	210.0
		elstat	−164.0	−142.7	−146.9	−129.4
		total	232.5	127.7	108.4	80.5
	E_{orb}	E_σ	−399.7	−211.1	−175.2	−128.9
		E_π	−67.7	−83.7	−83.1	−78.5
		total	−467.4	−294.8	−258.3	−207.4
	BE		144.7 (127;[b] >138[c])	102.7	88.6	71.3
$ReCl_4E$	E_{prep}	E_{prep} $ReCl_4$	32.5	32.7	32.1	32.0
		total	98.9	73.5	69.1	63.8
	E_{st}	Pauli	370.3	249.3	232.6	190.8
		elstat	−143.3	−119.9	−121.5	−105.8
		total	227.0	129.3	111.1	85.0
	E_{orb}	E_σ	−378.7	−197.7	−163.2	−118.7
		E_π	−69.1	−89.7	−89.5	−86.4
		total	−447.8	−287.4	−252.7	−205.1
	BE		121.9 (132−149;[d] 120−141[e])	84.6	72.5	56.3

[a] Values in kcal mol^{-1}. [b] Reference 13g. [c] Reference 13c. [d] Reference 13d. [e] References 13h,i. [f] BE = $-(E_{prep} + E_{st} + E_{orb})$.

Accurate experimental estimates of gas phase metal−chalcogen bond energies are rare and limited to oxygen. We are aware of only two direct determinations based on modern techniques. Thus, Hildenbrand[13f] et al. have determined the O_3-Os−O dissociation energy as 104 kcal mol^{-1} compared to our calculated value of 103.7 kcal/mol, Table 2. Watson[13e] et al. reported a value of 101 kcal mol^{-1}, in good agreement with our value and with Hildenbrand's,[13f] while Holm and Donahue[13g] reported a value of 73 kcal mol^{-1}, which is 30 kcal mol^{-1} lower than that of the other two experimental estimates.

In the second example, Gable[32] et al. determined a value of 116.8 ± 1.2 kcal/mol for the $(C_6Me_5)(O)_2Re$−O dissociation energy compared to our estimate of 118.5 kcal/mol for the $(C_6H_5)(O)_2Re$−O bond energy. Although our validation is limited due to the lack of accurate experimental data, it seems to indicate that BP86 can determine M−O bond energies with the error limit of 5 kcal/mol usually associated with metal−

(30) Fischer, J. M.; Piers, W. E.; Ziegler, T.; MacGillivray, L. R.; Zaworotko, M. J. *Chem. Eur. J.* **1996**, *2*, 1220.
(31) Sandblom, N.; Ziegler, T.; Chivers, T. *Can. J. Chem.* **1996**, *74*, 2363.
(32) Gable, K. P.; Juliette, J. J.; Li, C.; Nolan, S. P. *Organometallics* **1996**, *15*, 5250.

ligand bond energies calculated by this method. We expect a similar error margin for M−E bond energies involving the other chalcogens.

MCl_4E Complexes. The calculated M−E bond energies for the C_{4v} complexes MCl_4E (M = Cr, Mo, W, Re; E = O, S, Se, Te) are presented in Table 3. We find again that the metal to ligand σ-donation, $-E_\sigma$ of eq 4, in all cases contributes more to the M−E bond strength than the ligand to metal π back-donation, $-E_\pi$.

The σ-donation term, $-E_\sigma$, decreases in steps from oxygen to tellurium that reflect the incremental changes in the np_σ energies, Figure 2. The largest decrease is between oxygen and sulfur and the smallest decrease between sulfur and selenium. The ligand to metal π back-donation, $-E_\pi$, exhibits again a clear maximum for sulfur and selenium as the diffuse $5p_\pi$ orbitals of tellurium are unable to interact strongly with the d_π acceptor orbitals although the p_π to d_π energy gap is smallest for tellurium.

The selection of metal centers for the C_{4v} MCl_4E complexes includes one full transition metal triad (M = Cr, Mo, W) as well as two elements (M = W, Re) across the third transition series. We note within the group 6 triad that chromium on the top has the smallest $-E_\sigma$ contribution and the weakest M−E bond since its d_σ donor orbital, as expected, is of lowest energy. The $-E_\sigma$ contributions are similar for molybdenum and tungsten. The fact that $-E_\sigma$ and BE are slightly larger for tungsten can be attributed to the well-known relativistic stabilization for bonds involving 5d elements.[33] As we move along a transition series from tungsten to rhenium the d_σ donor orbital drops in energy with the increase in electronegativity (effective nuclear charge). The result is an expected reduction in $-E_\sigma$ and BE, Table 3.

Accurate experimental estimates of gas-phase metal−chalcogen bond energies for the Cl_4ME systems are even more rare than for the C_{3v} complexes and, again, are restricted to metal−oxygen bonds. Rappé and Goddard have carried out *ab initio* calculations[14a] on the Cr−O bond energy in Cl_4MO with only partial geometry optimization of the species involved. Their reported value of 82 kcal mol^{-1} is somewhat higher than our estimate of 69.8 kcal mol^{-1}. No experimental data are available for this complex.

Regarding the tungsten−oxygen bond dissociation energy in the WCl_4O complex, Holm and Donahue[13g] calculated a value of 127 kcal mol^{-1} from a thermodynamic cycle. On the other hand, Bryan and Mayer[13c] have provided a lower bound of 138 kcal mol^{-1} from a thermodynamic cycle involving a related complex with different ancillary ligands. Our calculated value is 144.7 kcal mol^{-1}. It should be noted that the suggested[13b] Cl_4W−O bond energy of 195.4 kcal mol^{-1} based on the electronegativity equilibration scheme due to Sanderson[13b] appears to be too high.

In the case of $MoCl_4O$, Holm and Donahue[13g] calculated a value of 101 kcal mol^{-1} from a thermodynamic cycle. On the other hand, Rappé and Goddard[14a] obtained an estimate of 102 kcal mol^{-1} based on *ab initio* calculations involving partial geometry optimization. The value obtained by us is 126.1 kcal mol^{-1}, Table 3.

An experimental value for the Cl_4Re−O bond energy is not available. However, there have been a number of estimates of the Re−O dissociation energy in $XReO_3$ type complexes.[13d,h,i,32] We note that our calculated value of 121.9 kcal mol^{-1} for the Cl_4Re−O bond energy is close to the experimental $Cp'(O)_2Re$−O bond energy of 116.8 kcal/mol determined by Gable et al.[32]

Concluding Remarks

We have studied the M−E bond for all members of the chalcogen family (E = O, S, Se, Te) in a series of metal compounds represented by the trigonal complexes OsO_3E and MCl_3E (M = V, Ta) and the square pyramidal systems MCl_4E (M = Cr, Mo, W. Re). All complexes were fully optimized, and the calculated geometrical parameters are in reasonable agreement with gas-phase electron diffraction data.[12]

Our ETS[16,17] analysis revealed that the strongest bonding interaction is due to the σ-donation, $-E_\sigma$, from the fully occupied d_σ donor metal orbital to the empty p_σ acceptor orbital on the chalcogen, Tables 2 and 3. The σ-donation and M−E bond energy decreases sharply from oxygen to sulfur, followed by a much smaller reduction between sulfur and selenium. The decrease in σ-donation and M−E bond energy continues between selenium and tellurium but at a higher rate. All these trends correlate well with the relative energies of the p_σ acceptor orbitals. The contribution, $-E_\pi$, from the chalcogen to metal π back-donation has a maximum for sulfur and selenium. However, in relative terms, the contribution from the π back-donation to the total M−E bond energy increases from oxygen to tellurium.

The role of the metal center was also analyzed by the ETS method. We find that both the σ-donation and the M−E bond energy decrease from bottom to top in a triad and from left to right in a transition metal series. Accurate experimental estimates of gas-phase metal−chalcogen bond energies are rare and limited to oxygen. Our calculated M−O bond energies in OsO_4 and $CpReO_3$ are in good agreement with very recent direct experimental measurements. Our values for the M−O bond energies in MCl_4O (M = Mo, W) are some 20 kcal/mol lower than the experimental estimates based on thermodynamical cycles.

We expect our DFT bond energies to be accurate to within 5 kcal/mol. Basis set superposition errors should be small due to the large size of our basis. Corrections due to finite temperature and zero point energy are not included in our calculations. We expect them to contribute with ±1−2 kcal/mol.

The scope of the present study has been limited to high-valent compounds in which the d_π orbitals are largely empty. We shall in a forthcoming study deal with low-valent systems where the d_π orbitals are nearly completely occupied.

Acknowledgment. Ò.G.B. gratefully acknowledges the Spanish Ministry of Education and Science for financial support. This investigation was supported by the Natural Sciences and Engineering Research Council of Canada (NSERC). We thank the Petroleum Research Fund administered by American Chemical Society (Grant ACS-PRF No. 31205-AC3) for further support of this research. A Canada Council Killam research fellowship to T.Z. is also acknowledged.

IC970613L

(33) Ziegler, T.; Snijders, J. G.; Baerends, E. J. *J. Chem. Phys.* **1981**, *74*, 1271.